

See discussions, stats, and author profiles for this publication at: <https://www.researchgate.net/publication/266262927>

Norbornene Oxidation by Chiral Complexes Encapsulated in NaY 2 Zeolite

ARTICLE in THE JOURNAL OF PHYSICAL CHEMISTRY C · AUGUST 2014

Impact Factor: 4.77 · DOI: 10.1021/jp5031812

READS

68

7 AUTHORS, INCLUDING:



Cesar J.S. Oliveira

University of Minho

31 PUBLICATIONS 422 CITATIONS

SEE PROFILE



Maria José Alves

University of Minho

75 PUBLICATIONS 457 CITATIONS

SEE PROFILE



Antonio Fonseca

University of Minho

73 PUBLICATIONS 917 CITATIONS

SEE PROFILE



Isabel Correia Neves

University of Minho

86 PUBLICATIONS 879 CITATIONS

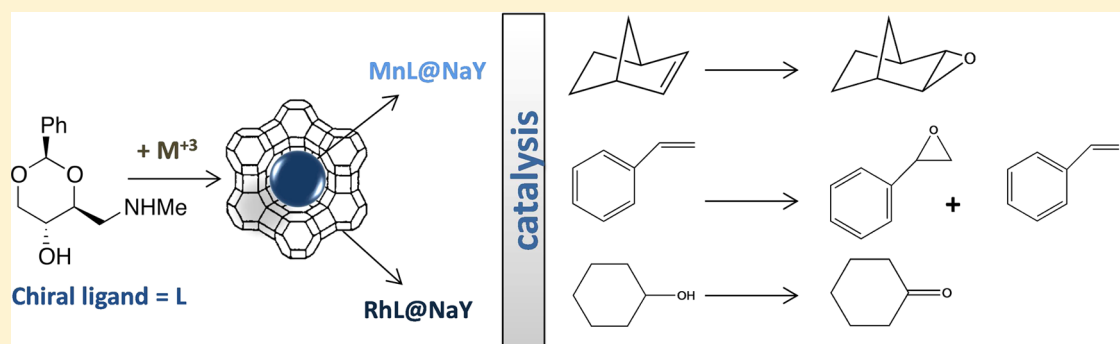
SEE PROFILE

Norbornene Oxidation by Chiral Complexes Encapsulated in NaY Zeolite

I. Kuźniarska-Biernacka,^{*,†} P. Parpot,[†] C. Oliveira,[†] A. R. Silva,[‡] M. J. Alves,[†] A. M. Fonseca,[†] and I. C. Neves^{*,†}

[†]Centro de Química, Departamento de Química, Universidade do Minho, Campus de Gualtar, 4710-057 Braga, Portugal

[‡]CICECO, Departamento de Química, Universidade de Aveiro, 3810-193 Aveiro, Portugal



ABSTRACT: The preparation of chiral metal complexes in NaY zeolite is reported. The guests, chiral metal complexes, were entrapped in the supercages of NaY zeolite (host) by a two-step process in the liquid phase: (i) inclusion of the selected transition metal (rhodium(III) and manganese(II)) by ion-exchange in the porous structure and (ii) introduction of the chiral ligand, an D-erythrose amino derivative, namely (2R,4S,5R)-4-[(N-methylamino)methyl]-2-phenyl-1,3-dioxan-5-ol, followed by assembly of the complex inside the void space of the zeolite. Structural (FTIR and XRD), surface studies (SEM) and chemical analyses were used to characterize the new host–guest catalysts and the results indicated that chiral metal complexes were successfully encapsulated in supercages of the NaY zeolite. Catalytic studies were performed in liquid phase for norbornene oxidation using *tert*-butyl hydroperoxide as the oxygen source. The catalytic results were compared with styrene and cyclohexanol oxidation as model reactions. The prepared chiral catalysts exhibited catalytic activity for all oxidation reactions. The stability of the catalysts before and after reaction was confirmed by cyclic voltammetry and FTIR studies.

INTRODUCTION

Catalytic enantioselective epoxidation of unfunctionalized alkenes, in which chiral recognition is based on nonbonding interaction between prochiral alkenes and chiral catalysts, has been receiving widespread attention.¹ This process provides a direct transformation of simple prochiral alkenes to enantio-enriched epoxides that are extremely versatile synthetic intermediates for construction of complex organic molecules.² Understanding the various factors affecting the enantioselectivity of the reactions will facilitate rational design for better catalysts. In the last decades, significant advances in enantioselective epoxidation of simple alkenes by applying the chiral Mn-Schiff base systems in the homogeneous phase have been made.^{3,4}

Studies by various groups have established the richness oxidation chemistry of oxomanganese complexes.^{4–8} In particular the reaction with alkenes is usually accompanied by large and negative entropies of activation.⁹ Therefore, it is possible that the introduction of chiral ligands to the metal coordination sphere results in enantioselective epoxidations. In the literature we found many examples for oxidation of styrene catalyzed by manganese 2,2'-bipyridine (bpy) complex cation

immobilized in Al-MCM-41,¹⁰ Salen type complexes immobilized in clays,¹¹ pillared clays (PILCs),^{12–14} zeolites,^{15,16} or polymers.¹⁷ Norbornene^{18,19} and secondary alcohols^{20,21} have also been oxidized in the presence of manganese-based catalysts. Less attention has been given to rhodium complexes in oxidation reactions.^{22,23} These results point out the success of olefins as well as oxidation of alcohols with manganese and rhodium complexes encapsulated into the NaY zeolite. The use of inorganic porous material has been high in the oxidation of organic compounds of large molecular sizes with a bulky oxidant such as *tert*-butyl hydroperoxide (tBuOOH).

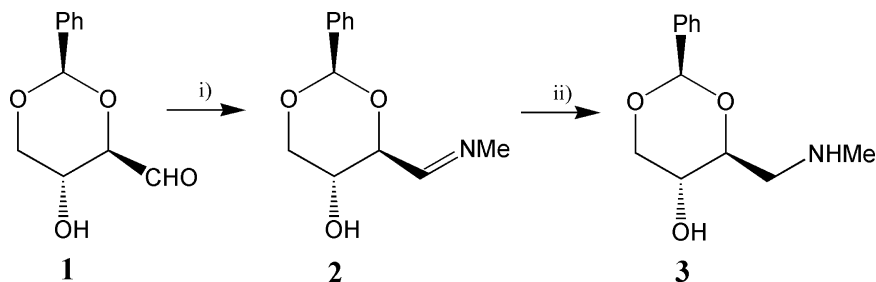
Numerous studies have been conducted on encapsulation of a variety of metal complexes^{24–29} and clusters³⁰ in zeolitic hosts. Likewise, the studies have been considered to improve the catalytic properties for these heterogeneous catalysts in the oxidation of different types of organic substrates with use of alternative oxidation processes based on low-toxicity oxidants. Some of these catalysts exhibit high activities in some

Received: March 31, 2014

Revised: July 31, 2014

Published: July 31, 2014



Scheme 1. Synthesis of Chiral Ligand 3^a

^aKey: (i) (a) THF, NH_2Me , 0 °C, 40 min; (b) rt, 2.5 h. (ii) MeOH, NaBH_4 , 0 °C, N_2 , 45 min.

industrially important reactions and possess the advantages of heterogeneous catalysis, such as easy separation and handling, efficient recycling, minimization of metal leaching, and in some cases higher selectivity than homogeneous catalysts.^{31,32}

In the present work, we aim to explore the catalytic ability of the prepared heterogeneous catalysts based on manganese or rhodium complexes with a chiral ligand for the oxidation of norbornene under mild conditions. Norbornene and its oxidation products like epoxynorbornene, diol, and others have wide applications in polymer synthesis, pharmaceutical intermediates, etc.³³ To achieve this goal, the NaY zeolite was used as a host for the encapsulation of the complexes prepared by a flexible ligand method in the liquid phase. The new heterogeneous catalysts were evaluated on the oxidation of norbornene by using *tert*-butyl hydroperoxide as the oxygen source and compared with styrene and cyclohexanol oxidations under mild conditions.

EXPERIMENTAL SECTION

Materials and Reagents. NaY zeolite (CBV100, Si/Al ratio = 2.83) in powder form was obtained from Zeolyst International. All other chemicals and solvents used were reagent grade and purchased from Aldrich: Carbon cement (Leit-C), Nafion, 2-hydroxyphenylaldehyde, manganese(II) chloride hydrate ($\text{MnCl}_2 \times 4\text{H}_2\text{O}$), rhodium(III) chloride hydrate ($\text{RhCl}_3 \times 3\text{H}_2\text{O}$), triethylamine, methylamine, acetonitrile, dichloromethane, ethanol, *tert*-butyl hydroperoxide solution 5.0–6.0 M in decane (*t*BuOOH), chlorobenzene (PhCl), styrene, norbornene, cyclohexanol, and sodium borohydride. Methanol and tetrahydrofuran were dried prior to use, from calcium hydrate and sodium/benzophenone, respectively. Potassium bromide used for the FTIR pellets preparation was purchased from Merck, spectroscopic grade. Toray carbon was obtained from Quintech. D-Erythrose benzylidene acetal (**1**) was prepared in two steps from D-glucose by the standard method.^{34,35}

Synthesis of the Chiral Ligand. The chiral ligand, D-erythrose amino derivative **3**, (2*R*,4*S*,5*R*)-4-[(*N*-methylamino)-methyl]-2-phenyl-1,3-dioxan-5-ol, was prepared in two steps from 2,4-*O*-benzylidene-D-erythrose acetal **1** (Scheme 1).^{34–36}

(a) A suspension of aldehyde **1** (0.210 g, 1.00 mmol) in dry THF (2 mL) was refrigerated at 0 °C, then methylamine was bubbled through for 40 min. The reaction mixture was kept at room temperature for an additional period of 2.5 h. Volatiles were removed in the rotary evaporator to give a white solid identified as imine **2** in quantitative yield. Mp 90–92 °C; $[\alpha]_{20}^{\text{D}} = +38.5^\circ$ (concn 0.93% MeCO_2Et); IR ν_{max} (Nujol, cm^{-1}) 3265 s, 1677 m; ^1H NMR (400 MHz, CDCl_3) δ 7.87 (1H, t, $J = 1.6$ Hz, H-1'), 7.54–7.38 (5H, m, H-Ph), 5.57 (1H, s, H-2), 4.37

(1H, dd, $J = 5.2, 10.8$ Hz, H-6), 4.14 (1H, dt, $J = 1.6, 8.8$ Hz), 4.02–3.96 (1H, m, H-5), 3.71 (1H, t, $J = 10.8$ Hz, H-6), 3.35 (3H, s, H-3') ppm; ^{13}C NMR (100.62 MHz, CDCl_3) δ 166.4 (C-1'), 137.2 (Cq-Ph), 129.1 (CH-Ph), 128.3 (CH-Ph), 126.1 (CH-Ph), 101.4 (C-2), 79.9 (C-4), 70.2 (H-6), 64.9 (H-5), 47.3 (C-3') ppm; HRMS (ESI) calcd 222.1125 [$(\text{C}_{12}\text{H}_{16}\text{NO}_3)^+$], obtained 222.1123.

(b) The imine **2** (0.109 g, 0.49 mmol) was dissolved in dry methanol (5 mL) and the solution was stirred under N_2 and cooled to 0 °C. Sodium borohydride (0.040 g; 1.08 mmol) was added in one portion and the reaction was allowed to run for another 45 min. The solvent was evaporated, then the residue was redissolved in ethyl acetate (20 mL) and washed with H_2O (10 mL). The aqueous solution was extracted with ethyl acetate (2×20 mL). The organic extracts combined were dried over MgSO_4 and filtered, then the solvent was evaporated under vacuum to give ligand **3** as a colorless oil in quantitative yield. $[\alpha]_{20}^{\text{D}} = -51.8^\circ$ (concn 1.28%; MeCO_2Et); IR ν_{max} (Nujol, cm^{-1}) 3316 s, 3067 s, 1462 s, 1380 s; ^1H NMR (400 MHz, CDCl_3) δ 7.51–7.49 (2H, m, H-Ph), 7.36 (3H, dd, $J = 2.0, 5.2$ Hz, H-Ph), 5.56 (1H, s, H-2), 4.23 (1H, dd, $J = 4.8, 10.4$ Hz, H-6), 3.80 (1H, td, $J = 2.8, 8.8$ Hz, H-4), 3.63 (1H, t, $J = 10$ Hz, H-6), 3.54 (1H, td (distorted td with $J = 8.8$ and 10 Hz), $J = 4.8, 8.8, 10$ Hz, H-5), 3.13 (1H, dd, $J = 2.8$ Hz, 12.8 Hz, H-1'), 2.87 (1H, dd, $J = 8.4, 12.8$ Hz, H-1'), 2.48 (3H, s, H-3') ppm; ^{13}C NMR (100.62 MHz, CDCl_3) δ 139.3 (Cq-Ph), 129.9 (CH-Ph), 129.1 (CH-Ph), 127.4 (CH-Ph), 102.3 (C-2), 81.2 (C-4), 72.2 (C-6), 64.8 (C-5), 53.2 (C-1'), 35.8 (C-3') ppm; HRMS (ESI) calcd 224.1281 [$(\text{C}_{12}\text{H}_{18}\text{NO}_3)^+$], obtained 224.1284.

Preparation of Chiral Complexes Encapsulated in NaY. The heterogeneous catalysts were prepared by encapsulation of the selected transition metal (Rh(III) or Mn(II)) by ion-exchange in the zeolite structure, followed by diffusion of chiral ligand, (2*R*,4*S*,5*R*)-4-[(*N*-methylamino)-methyl]-2-phenyl-1,3-dioxan-5-ol, in M-NaY host, based on a previously established procedure.^{37–42} The resulting catalysts were purified by Soxhlet extraction with appropriate organic solvent to remove unreacted ligand and residual complexes adsorbed onto the external surface of the zeolite crystallites. Finally, the samples were dried in an oven at 60 °C, under vacuum, for 12 h. The solid samples were denoted as ML@NaY, where L represents the chiral ligand, the D-erythrose amino derivative, and M the transition metal selected.

Synthesis of MnL@NaY. An aqueous solution containing 0.034 g (0.170 mmol) of $\text{MnCl}_2 \times 4\text{H}_2\text{O}$ was added to 1.50 g of NaY (previously dried at 120 °C) and the mixture was further stirred for 24 h at room temperature. The solid fraction was filtered out and dried at 120 °C for 12 h. A solution of chiral ligand (0.031 g, 0.140 mmol) was stirred with Mn–Y in 25 mL

of ethanol during 24 h at room temperature. The resulting mixture was filtered and washed with dichloromethane. After 6 h of Soxhlet extraction with dichloromethane, the catalyst was dried in an oven at 90 °C, under vacuum, for 12 h. The color of MnL@Y obtained is pale beige (Mn, 0.47% wt).

Synthesis of RhL@NaY. An analogous procedure was followed for preparing RhL@NaY. A solution of $\text{RhCl}_3 \times 3\text{H}_2\text{O}$ (0.046 g, 0.175 mmol) was added to 1.5 g of dry NaY host. After 24 h of stirred at room temperature, Rh–Y was filtered off and washed with dichloromethane. A solution of chiral ligand (0.031 g, 0.140 mmol) was added to dry Rh–Y, and this mixture was stirred for 24 h at room temperature. After Soxhlet extraction for 6 h with ethanol and being dried in an oven at 90 °C, under vacuum, for 12 h, the pale orange RhL@Y catalyst is obtained (Rh, 0.15% wt).

Preparation of Zeolite-Modified Electrodes. The preparation of the zeolite-modified electrodes was based on a previous established procedure.⁴³ To prepare the zeolite-modified electrodes, 20 mg of the heterogeneous catalysts (as prepared and after norbornene oxidation reaction) was suspended in a Nafion/water solution (120 μL Nafion/120 μL ultrapure water). The resulting solutions were homogenized by using an ultrasound bath and deposited on carbon Toray paper with an area of $2 \times 2 \text{ cm}^2$. The carbon was used to increase the area of electrical conductor in direct contact with the zeolite. Finally, the carbon Toray paper was glued to the platinum electrode by using conductive carbon cement and dried at room temperature for 24 h.

Characterization. The chemical analysis of parent zeolite and the heterogeneous catalysts was carried out by Inductively Coupled Plasma Atomic Emission Spectrometry (ICP-AES), using a ICP-AES Horiba Jobin-Yvon model Ultima Spectrometer with SMEWW 3120 method, after acid digestion of the samples in “Laboratório de Análises” of the Instituto Superior Técnico (Portugal). Elemental analysis for carbon, nitrogen, and hydrogen was carried out with a LECO CHNS-932 analyzer. The samples were combusted at 1000 °C for 3 min with helium used as the purge gas. NMR spectra were obtained with a Varian Unity Plus spectrometer at an operating frequency of 300 MHz for ^1H NMR and 75.4 MHz for ^{13}C NMR or with a Bruker Avance III 400 at an operating frequency of 400 MHz for ^1H NMR and 100.6 MHz for ^{13}C NMR. All chemical shifts are given in ppm, using δ_{H} $\text{Me}_4\text{Si} = 0$ ppm as reference, and J values are given in Hz. Assignments were made by comparison of chemical shifts, peak multiplicities, and J values and were supported by spin decoupling double resonance and bidimensional heteronuclear HMBC and HMQC correlation techniques. Mass spectrometry analyses were performed at the “C.A.C.T.I. - Unidad de Espectrometría de Masas” at the University of Vigo, Spain. FTIR spectra were recorded in the range 4000–500 cm^{-1} with a Bomem MB104 spectrophotometer by averaging 32 scans at a maximum resolution of 4 cm^{-1} . The FTIR spectrum of the ligand was obtained in Nujol and the spectra of solid samples were obtained from powdered samples mixed with KBr. Phase analysis was performed by X-ray diffraction (XRD) with a Philips PW1710 diffractometer. Scans were taken at room temperature in a 2θ range between 5 and 60°, using $\text{Cu K}\alpha$ radiation. Scanning electron micrographs (SEM) were collected with a LEICA Cambridge S360 scanning microscope equipped with an EDX system. To avoid surface charging, samples were coated with gold under vacuum prior to analysis, by using a Fisons Instruments SC502 sputter coater. Cyclic voltammetry

measurements zeolite based materials were carried out by using a computerized AMEL instrument General-purpose Potentiostat model 2051. The experimental were controlled with a homemade program LAB VIEW. All electrochemical studies were performed at room temperature with a three-electrode assembly that included a 250 mL glass cell, a saturated calomel electrode as reference electrode, and a 90% platinum and 10% iridium counter electrode. The working electrode was carbon Toray (CT) or CT modified by heterogeneous catalysts before and after catalytic reaction. The thermal stability of the heterogeneous catalysts was determined by thermogravimetric analysis in a STA 409 PC/4/H Luxx Netzsch thermal analyzer. The atmosphere used was high-purity air (99.99% minimum purity) with a flow rate of 50 mL/min. The sample holders used were crucibles of aluminum oxide, supplied by Netzsch. The samples were heated between 50 and 700 °C at 10 deg/min to evaluate the thermal stability.

Catalytic Oxidation. Catalytic oxidation was carried out in a 50-mL round-bottomed flask equipped with a condenser and a magnetic stirrer. In a typical batch, the reactor was charged with 100 mg of the catalysts, previously activated in an oven at 120 °C under vacuum for 12 h. The $t\text{BuOOH}$ (oxygen source) was added to the reactor under stirring by a KD Scientific Syringe Pump: KDS 200P. After the reaction cycle, the heterogeneous catalysts were washed, dried, and characterized. Samples of the reaction mixture were withdrawn at fixed time intervals and analyzed by gas chromatography. To identify the enantiomer/diastereomer products, GC analyses of the norbornene and styrene oxidation reactions were carried out in different GC-FID. The samples of the reaction mixture were analyzed by GC-FID (using the internal standard method) on a Varian 450 GC gas chromatograph equipped with a fused silica Varian Chrompack capillary column VF-5 ms (15 m \times 0.25 mm id; 0.15 μm film thickness), using helium as carrier gas (retention times: 4.0 min *endo*-epoxynorbornane, 4.4 min *exo*-epoxynorbornane, 4.6 min benzaldehyde, 6.5 min phenylacetaldehyde, and 7.2 min styrene epoxide). The styrene epoxide enantiomeric excesses (% ee) were determined in the same chromatograph but with use of a fused silica Varian Chrompack capillary column CP-Chiralsil-Dex CB (25 m \times 0.15 mm d.i. \times 0.25 μm film thickness). The several chromatographic peaks were identified against commercially available or synthesized samples and/or by GC-MS (Finnigan Trace). However, the GC-FID chromatograms of products obtained from norbornene, styrene, and cyclohexanol oxidations were obtained in a SRI 8610C chromatograph with use of nitrogen as carrier gas, equipped with a CP-Sil 8CB capillary column, and a FID detector. The different substrates and products were qualitatively and quantitatively determined (by the internal standard method). The identification of reaction products was confirmed by GC-MS (Varian 4000 Performance). After the reaction cycle, the catalysts were washed, dried, and characterized. All blank experiments with NaY as catalyst were performed under the same reaction conditions.

Oxidation of Norbornene. The oxidation of norbornene was studied at 50 °C under constant stirring. Briefly, norbornene (1.0 mmol), chlorobenzene (1.0 mmol, internal standard), and heterogeneous catalyst (0.10 g) were mixed in acetonitrile (4.0 mL). The oxygen source, $t\text{BuOOH}$ (0.2 mL of 5.5 M in decane solution), was progressively added to the reaction medium. The reaction products were analyzed and identified as mentioned above.

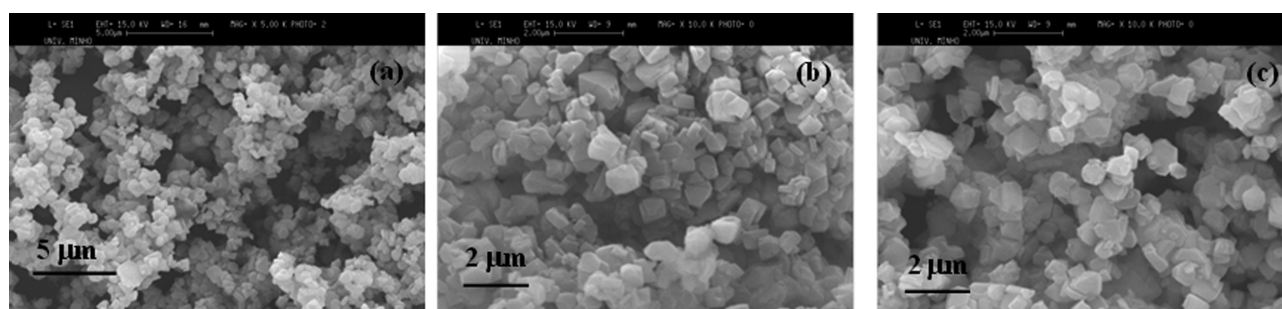


Figure 1. SEM micrographs of (a) NaY, (b) RhL@Y, and (c) MnL@Y with different resolutions.

Oxidation of Styrene. The epoxidation of styrene was studied at room temperature under constant stirring. Briefly, styrene (1.0 mmol), chlorobenzene (0.1 mmol, internal standard), and heterogeneous catalyst (0.10 g) were mixed in acetonitrile (5.0 mL). The *t*BuOOH (0.3 mL of 5.5 M in decane solution) was progressively added to the reaction medium. The reaction products were analyzed and identified as mentioned above.

Oxidation of Cyclohexanol. The reaction was carried out in acetonitrile (4.0 mL) at $40(\pm 5)$ °C with constant stirring, and the composition of the reaction medium was the following: cyclohexanol (0.6 mL, 5.8 mmol), chlorobenzene (0.6 mL, 5.9 mmol (internal standard)), and heterogeneous catalyst (0.10 g). The oxidant, *t*BuOOH (2 mL of 5.5 M in decane solution), was progressively added to the reaction medium. The reaction products were analyzed and identified as mentioned above.

RESULTS AND DISCUSSION

Characterization of Catalysts. The metal complexes into the NaY zeolite supercages were synthesized in situ performed by a flexible ligand method in the liquid phase. The ligand used is a chiral compound, a D-erythrose amino derivative, bearing oxygen and nitrogen donor atoms in its structure necessary to obtain stable and active chiral complexes into the NaY for norbornene oxidation. The catalytic results were compared with those obtained from styrene and cyclohexanol oxidations.

The results from different characterization techniques reveal the unequivocal evidence for the encapsulation of chiral metal complexes in the supercages of the NaY zeolite. The morphology of the samples was determined by scanning electron microscopy (SEM) analysis. Figure 1 shows the field emission scanning electron micrographs of the parent zeolite and the heterogeneous catalysts.

Analysis of the SEM micrographs of the NaY and the heterogeneous catalysts shows the typical morphology of faujasite zeolite and no significant differences were found. The parent zeolite presents well-formed cubic particles with an average size of about 0.6–0.8 μm. The average particle size after encapsulation of the chiral complexes reminds unchanged, indicating that there are no changes in the zeolite morphology upon encapsulation of the chiral complexes.^{24,25}

Preservation of the zeolite structure of the samples was monitored by X-ray powder diffraction (XRD). The powder XRD patterns of MnL@Y, RhL@Y, and NaY are shown in Figure 2. These samples displayed the expected pattern of hydrated NaY zeolite and no diffraction lines assigned to any new phase were detected.⁴⁴

There is an empirical relationship between the relative intensities of 331, 311, and 220 peaks and cation location in faujasite-type zeolites.^{44,45} Cations are randomly distributed

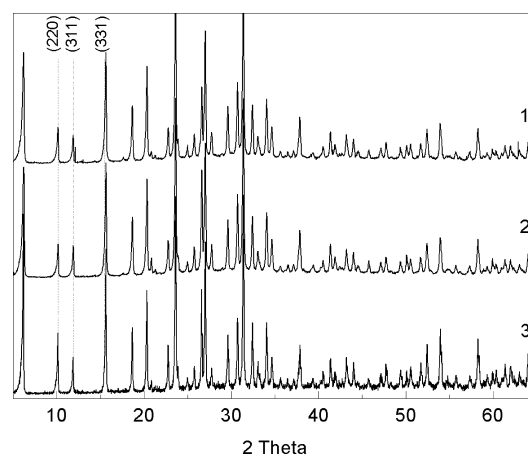


Figure 2. XRD patterns of (1) MnL@Y, (2) RhL@Y, and (3) NaY.

within the lattice if $I_{331} > I_{220} > I_{311}$, but if $I_{331} > I_{311} > I_{220}$, the cations assume positions at sites I' and II. The XRD patterns of both heterogeneous catalysts show some changes in the relative intensities of the 331, 311, and 220 peaks when compared to the NaY zeolite. In the parent zeolite retention of the random sodium ion location is assumed. However, analysis of the pattern of both catalysts indicates that some cation redistribution occurred following complex formation. We presume that this is an indication that both complexes displaced sodium ions from their random positions in the supercages to locations at sites I' and II.⁴⁶ Site I' is reportedly located in the sodalite cavity while site II is at the center of a single six-ring (S6R) or displaced from this point into supercages.⁴⁴

IR spectroscopy also is an additional characterization tool of the encapsulation of the complexes within NaY. FTIR spectra of NaY, M@Y (Mn or Rh), and the heterogeneous catalysts are displayed in Figure 3.

The FTIR spectra of all the samples are dominated by the strong bands attributed to the zeolite structure. The FTIR spectrum of the parent zeolite is characterized by a very intense broad band at around 3460 cm^{-1} with a shoulder at around 3600 cm^{-1} . The shoulder should be due to the hydroxyl groups in the supercages and in the sodalite cages, respectively.^{47,48} In the low-energy region the spectrum shows a band at 1640 cm^{-1} characteristic of the $\delta(\text{H}_2\text{O})$ mode of absorbed water.⁴⁹ The band at around 1020 cm^{-1} is usually attributed to the asymmetric stretching of the Al–O–Si chain of zeolite. The symmetric stretching and bending frequency bands of the Al–O–Si framework of zeolite appear at 727 and 513 cm^{-1} , respectively.⁵⁰ FTIR spectra of both M–Y and the ML@Y are dominated by the strong bands attributed to the zeolite

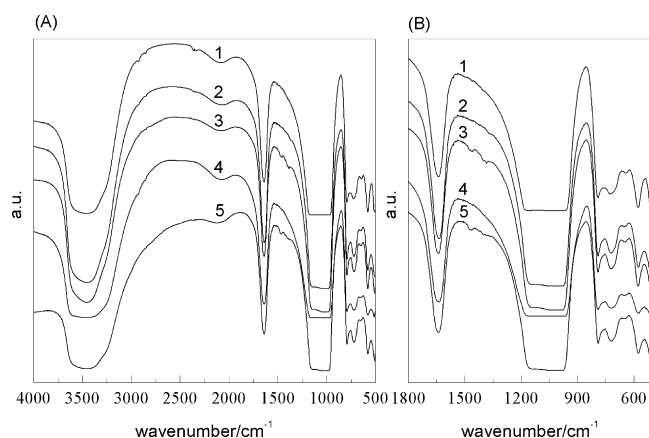


Figure 3. FTIR spectra of (1) NaY, (2) Mn@Y, (3) MnL@Y, (4) Rh@Y, and (5) RhL@Y in the range (A) 4000–500 and (B) 1800–500 cm^{-1} .

structure. No shift or broadening of the zeolite vibration bands is observed upon encapsulation of the complexes. The ion-exchange treatment does not modify the zeolite structure. As expected, in addition to the strong bands caused by the parent zeolite, the spectra of MnL@Y and RhL@Y also show bands in the 1600–1200 cm^{-1} region, where the parent zeolite does not absorb, which are attributed to the presence of the complexes. Due to the low concentration of metal complex inside the zeolite, only the low-intensity bands at 1465 and 1385 (sh) cm^{-1} are observed and are attributed to the encapsulated complexes.

The results of chemical analyses of MnL@Y and RhL@Y catalysts confirmed the presence of metal complexes in the zeolite framework. Different metal loading was observed for the encapsulated manganese and rhodium complexes with 85.5 and 14.6 $\mu\text{mol/g}$, respectively. The parent zeolite and both heterogeneous catalysts show the same molar Si/Al ratio which differs between 2.83 to 2.85, indicating that no dealumination occurs during the in situ encapsulation. Rh/Si and Mn/Si ratios obtained for both catalysts are 0.0015 and 0.0090, respectively, which corresponds to 0.21 molecules of Rh per unit cell (UC) and 1.26 Mn/UC. The value obtained for rhodium per UC is similar to that found for (*N,N'*-diarylacetamidine)rhodium(III) complex encapsulated into the zeolite Y.⁴³ The C/N ratio obtained for both heterogeneous catalysts (10.15 and 10.20 for manganese and rhodium complexes, respectively) is similar to the theoretical value observed for neat complex (10.30), indicating that the chiral ligand structure is not affected by diffusion/complexation. However, the M/N ratio obtained for both heterogeneous catalysts was 3.49 and 2.00 for Rh/N and Mn/N, respectively, suggesting that only one type of complex with a stoichiometry 1:2 was achieved.

The presence of the complexes in the zeolite was confirmed also by thermal gravimetric analysis (TGA). The TGA curve of the parent zeolite shows a significant weight loss from 60 to 200 $^{\circ}\text{C}$, with the maximum around 150 $^{\circ}\text{C}$, attributed to the removal of intrazeolite water. Both heterogeneous catalysts present similar TGA profiles in the studied temperature range (50–700 $^{\circ}\text{C}$). Two distinct weight changes are seen in the TGA data for both catalysts. A major stage of weight loss from 60 $^{\circ}\text{C}$ to around 200 $^{\circ}\text{C}$, with the maximum at 160 $^{\circ}\text{C}$, was due to the contributions from the physisorbed water within the zeolite structure and the other, in the range 300–450 $^{\circ}\text{C}$, was related to the onset of decomposition of the organic moiety from the complex. With the increase of temperature, the weight loss observed is associated with progressive decomposition of the encapsulated complexes.

According to the results previously discussed, it can be assumed that the complexes are located inside the zeolite pore structure.

Catalytic Studies. The catalytic studies of chiral complexes encapsulated in NaY were performed in the liquid phase for norbornene oxidation, using *tert*-butyl hydroperoxide as the oxygen source. These results were compared with those of styrene and cyclohexanol oxidation as model reactions. For all oxidation reactions, the parent zeolite and M-NaY ($M = \text{Rh}$ or Mn) show the same performance with a residual conversion ($\leq 5\%$). The presence of the chiral complexes encapsulated in NaY improved the catalytic activity of the heterogeneous catalysts. The typical products of norbornene oxidation are epoxynorbornane, norbornanone, and norborneol (Figure 4).^{33,51,52} The 3-cyclohexene-1-carboxaldehyde was also detected in acidic media as a result of rearrangement of *exo*-2,3-epoxynorbornane.⁵³ When *t*BuOOH was used as an oxygen source in the presence of cobalt-based catalyst, epoxynorbornane and peroxonorbornyl radical were detected.^{54,55} Under specific conditions, in the presence of group VIII transition metal carbene complexes in protic media, norbornene opens followed by polymerization.⁵⁶

In this work the norbornene opening products were not detected, most probable due to reaction conditions used: aprotic solvent (acetonitrile) and the oxygen source (*t*BuOOH). Both chiral heterogeneous catalysts show high substrate conversion, more than 80% (Table 1). These experiments were duplicated and the results were found to be reproducible with a maximum error of ca. 1% relative to the substrate conversion average. Norbornene oxide was identified by mass spectrometry. All ions in the m/z range 50–400 were examined, and compound identification was based on comparison of the resulting spectra with mass spectral libraries (NIST/EPA/NIH 2008 and Wiley Registry sixth Edition). Thus, m/z 110 was identified as the daughter ion, corresponding to $\text{C}_7\text{H}_{10}\text{O}$ (epoxide). Analysis of the epoxynorbornane by GC-MS confirms that 99% is the *exo* isomer

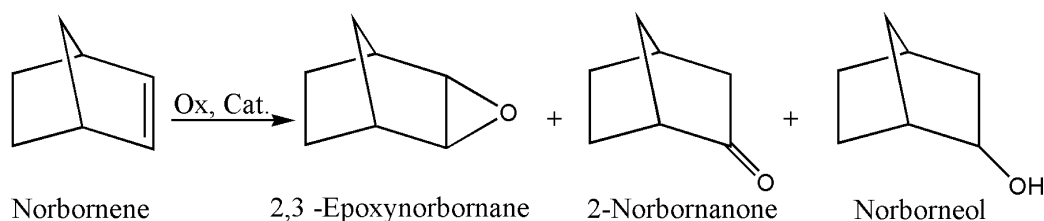


Figure 4. Common products of norbornene oxidation.

Table 1. Oxidation of Organic Molecules Catalyzed by MnL and RhL Complexes Encapsulated into Zeolite Y

substrate	entry	catalyst	t (h) ^a	% C ^{b,c}	% S _{product} ^{b,d}	% η _{product} ^{b,e}
norbornene	1	NaY	48	5	100 ^f	5
	2	MnL@Y	48	83	100 ^f	83
	3	RhL@Y	48	82	100 ^f	82
styrene	4	NaY	48	4	0 ^{g,h}	0 ^{g,h}
	5	MnL@Y	48	52	17 ^{g,i}	9 ^{g,i}
	6	RhL@Y	>48	18	ND ^j	ND ^j
cyclohexanol	7	NaY	48	3	100 ^k	3
	8	MnL@Y	24	55	100 ^k	55
	9	RhL@Y	<24	27	100 ^k	27

^aReaction time at which the substrate conversion starts to become constant. ^bDetermined by GC against an internal standard. ^cSubstrate conversion (C) calculated as $C = \{[A_{(\text{substrate})}/A_{(\text{PhCl})}]_{t=0h} - [A_{(\text{substrate})}/A_{(\text{PhCl})}]_{t=xh}\} \times 100/[A_{(\text{substrate})}/A_{(\text{PhCl})}]_{t=0h}$. ^dProduct selectivity (S) calculated as $S = A_{(\text{product})}/[A_{(\text{product})} + A_{(\text{other products})}]$, in which A is the chromatographic peak area. ^eProduct yield (η) calculated as $\eta = CS/100$. ^fEpoxyornobornene. ^gStyrene epoxide. ^hOther products: % $S_{\text{benzaldehyde}} = 100$, % $\eta_{\text{benzaldehyde}} = 4$. ⁱOther products: % $S_{\text{benzaldehyde}} = 77$, % $\eta_{\text{benzaldehyde}} = 40$, % $S_{\text{phenylacetaldehyde}} = 6$, % $\eta_{\text{phenylacetaldehyde}} = 3$. ^jNo products were detected by GC. ^kCyclohexanone.

and only 1% the *endo*-epoxyornobornene isomer. The retention time of these isomers was also confirmed by synthesizing the epoxyornobornene, using *m*-chloroperbenzoic acid, to confirm the configuration of the isomers. From the literature, the selectivity and yield of epoxide are moderate and most of the authors do not specify the epoxy isomer obtained.^{33,51,57,58} The chiral iron(III)-Salen catalysts were found to be selective to *exo*-epoxyornobornene with moderate yield (21–35%).⁵⁹ When mesoporous materials were used as catalysts under similar conditions used in our work (oxygen source and solvent), the main product identified was *exo*-2,3-epoxyornobornene and its selectivity was 61–87%.⁵² Similar results were obtained with other systems based in mesoporous materials with high selectivity (89–99%) for the *exo* isomer.⁶⁰

The catalytic activity of manganese complexes encapsulated into the zeolite Y in the epoxidation of styrene reaction has been confirmed by many authors.^{61–63} Especially, Mn(III) complexes with Schiff bases show high activity in the presence of *t*BuOOH.^{64,65} The rhodium mixed ligand complexes also act as homogeneous catalysts in the oxidation of styrene.^{67,68} The major product of this reaction was benzaldehyde with minor amounts of the epoxide, phenyl methyl ketone,⁶⁸ and *tert*-butyl alcohol,⁶⁷ when *t*BuOOH was used as the oxygen source. The literature data show that the temperature has an influence on the styrene conversion. A dramatic decrease of substrate conversion (ca. 40%) was observed when the temperature decreases by 20 °C, whereas the distribution of products stays unchanged.¹⁵ Usually the reaction is not selective and leads to benzaldehyde (main product), styrene epoxide, and phenylacetaldehyde.^{15,69–71}

In the present study, the styrene oxidation occurs at room temperature (Table 1). These catalytic results confirm that manganese complex is active in the heterogeneous oxidation of styrene, as parent zeolite does not show significant conversion of substrate. The main product of this reaction is benzaldehyde. A small amount of styrene epoxide (% $S = 17$) and phenylacetaldehyde (% $S = 6$) was also detected whereas the phenyl-1,2-ethanediol was not. No enantioselectivity was observed in the styrene epoxide synthesis. The product

distribution is in agreement with literature data^{69–71} of styrene oxidation in the presence of MnSalen-based catalysts in the heterogeneous phase. The significant differences in styrene conversion reported in the literature (95–80%) and those obtained in this work (52%) are probably due to the experimental conditions used. In this work, the reaction runs at room temperature, and the conversion obtained is close to results at 50 °C (% $C = 43$), when MnSalen@NaY was used.¹⁵

The RhL@Y catalyst leads to low styrene conversion and no products were detected by GC. These results could be due to the reaction between rhodium species and styrene (olefin activated by the π -electron-withdrawing group), to form the rhodium–styrene π -complex.^{72,73} The formed π -complex is stable⁷³ and cannot effectively pass through the zeolite framework. Nevertheless, some adsorption of the substrate cannot be excluded. To support this statement, the oxidation of cyclohexanol, as an example of the molecules without a π -electron-withdrawing group, was studied.

The oxidation of cyclohexanol is negligible in the absence of heterogeneous transition metal catalysts confirming that under the experimental conditions, the oxidation is indeed catalytic in nature. The parent zeolite NaY is also catalytically inactive (Table 1). Therefore, the determining role is played by chiral metal complexes encapsulated into the zeolite. Our results show an enhancement of the conversion percentages to 27% and 55% in the presence of RhL@Y and MnL@Y, respectively. Only cyclohexanone was detected by GC as a product of cyclohexanol oxidation in both reactions. The presence of cyclohexanone in the reaction medium, when RhL@Y was used as a catalyst, supports the statement mentioned above that only the RhL– π -styrene complex is formed inside NaY.

The stability of the heterogeneous catalysts before and after oxidation reactions was determined by cyclic voltammetry studies. This technique is an important tool for displaying the presence of redox-active species inside the zeolite framework and their stability.^{26,41,43,74,75} Zeolite-encapsulated metal complexes were deposited on carbon Toray (CT) to determine the electroactivity and the stability of the metal complex by cyclic voltammetry. The voltammetry studies were carried out in 0.10 M NaCl aqueous medium, at room temperature. When the modified electrodes were placed in the electrolytic solution and washed, no change in the color of the solution was observed before and after oxidation reactions. Under our experimental conditions the modified electrodes are mechanically and chemically stable.^{26,41,43}

The cyclic voltammograms of the parent zeolite-modified electrode NaY-CT (Figure 5a) exhibit no redox processes in the scan potential of –0.50 to 1.40 vs SCE. However, all heterogeneous catalyst-modified electrodes before and after oxidation of olefins and cyclohexanol reactions exhibit redox processes in this range of potential. These results were attributed to the redox activity of the metal complexes located in the zeolite supercages.

The cyclic voltammograms obtained with the MnL@Y/CT modified electrode before and after norbornene oxidation are depicted in Figure 5 as an example.

The cyclic voltammograms show an anodic process at 0.90 V vs SCE with cathodic counterpart at 0.58 V vs SCE. The potential of the peak obtained from the cyclic voltammograms of the MnL@Y before reaction (Figure 5b) matches well with that of the MnL@Y after reaction (Figure 5c). Also, the cyclic voltammograms obtained with RhL@Y/CT zeolite-modified electrode before and after catalytic reactions are very similar

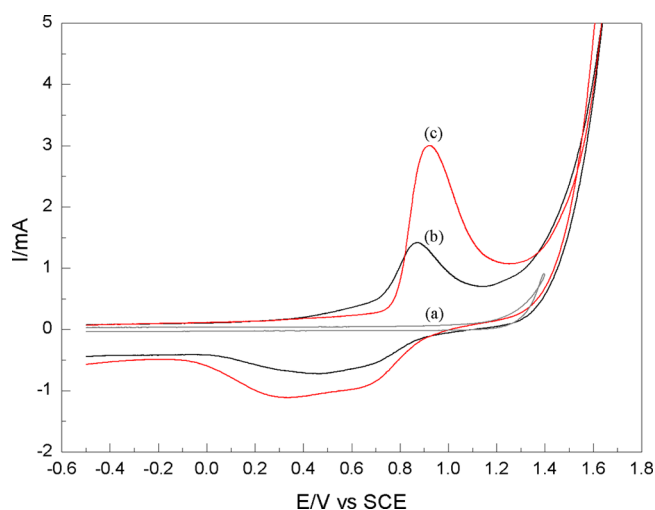


Figure 5. Cyclic voltammograms for NaY/CT (a) and MnL@Y/CT before (b) and after (c) norbornene oxidation with a scan rate 0.10 V s^{-1} in different potential ranges taken in water with 0.1 M NaCl as the supporting electrolyte.

and show a process at $0.20\text{--}0.08 \text{ V}$ vs SCE. These results indicate that both heterogeneous catalysts after the catalytic reaction maintain the molecular structure of the metal complexes. In addition the information about the stability of the heterogeneous catalysts used in the oxidation of olefins and cyclohexanol can be obtained from FTIR analysis.

Figure 6 presents the FTIR spectra of the heterogeneous catalysts obtained after the second reaction run for the oxidation of olefins and cyclohexanol.

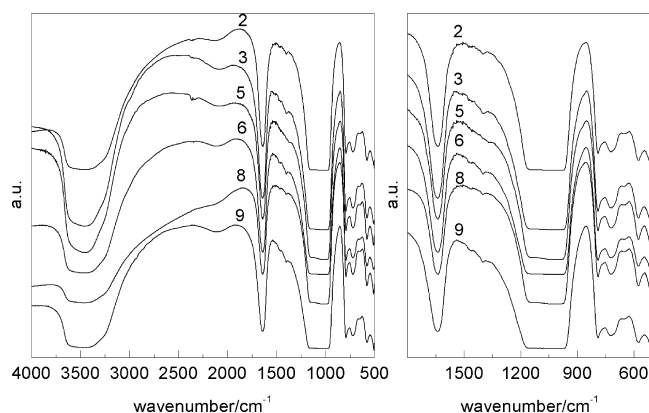


Figure 6. FTIR spectra in the range (A) $4000\text{--}500$ and (B) $1800\text{--}500 \text{ cm}^{-1}$ for MnL@Y and RhL@Y catalysts after the second catalytic tests. Numbers correspond to the entries in Table 1.

The FTIR spectra of all catalysts showed bands in the $1620\text{--}1200 \text{ cm}^{-1}$ region, which is where bands due to the complex should appear. This suggests that there is no complex leaching or any complex degradation. No changes in the characteristic bands of NaY were detected after the catalytic reactions. Therefore, these results suggest that the complex structure is retained under the experimental conditions used and most probably it can be reused without any significant activity lost in agreement with electrochemical studies.

CONCLUSIONS

New chiral catalysts have been prepared by the flexible ligand method in the supercages of the zeolite NaY. The manganese and rhodium complexes with a chiral ligand, a D-erythrose amino derivative, were encapsulated. The new heterogeneous catalysts, RhL@Y and MnL@Y, have been studied in the catalytic epoxidation of norbornene, styrene, and cyclohexanol with use of *t*BuOOH as the oxygen source in acetonitrile. Both catalysts showed catalytic activity in these reactions and their catalytic behavior depends on the metal complex: MnL@Y shows higher substrate conversion than RhL@Y. Our results show that the chiral heterogeneous catalysts are totally stereoselective in the liquid-phase oxidation of norbornene to *exo*-epoxynorbornane.

AUTHOR INFORMATION

Corresponding Authors

*I.K.B.: E-mail: iwona@quimica.uminho.pt. Fax: +351-253604382. Tel: +351-253601552.

*I.C.N.: E-mail: ineves@quimica.uminho.pt.

Notes

The authors declare no competing financial interest.

ACKNOWLEDGMENTS

The authors thank Dr. M. F. R. Pereira for support in the TGA analysis. I.K.B., A.R.S., and C.O. thank the Foundation for the Science and Technology (FCT, Portugal), for the contract under “Programa Ciência 2007 e 2008”. A.R.S. also thanks FCT for the contract under “Investigador FCT 2012” and I.K.B. also is thankful for the contract under the project NORTE-07-0124-FEDER-000039. The authors thank the FCT and FEDER-COMPETE-QREN-EU for financial support to the Research Centers, CQ/UM, PEst-C/UI/0686/2013 (F-COMP-01-0124-FEDER-037302), the project NORTE-07-0124-FEDER-000039, the NMR Portuguese network (PTNMR, Bruker Avance III 400-University Minho), and CICECO/UA (Pest-C/CTM/LA0011/2013).

REFERENCES

- (1) Fung, W. H.; Yu, W.-Y.; Che, C. M. Mechanistic Investigation of the Oxidation of Aromatic Alkenes by Monooxoruthenium(IV). Asymmetric Alkene Epoxidation by Chiral Monooxoruthenium(IV) Complexes. *J. Org. Chem.* **1998**, *63*, 7715–7726.
- (2) Besse, P.; Veschambre, H. Chemical and Biological Synthesis of Chiral Epoxides. *Tetrahedron* **1994**, *50*, 8885–8927.
- (3) Jacobsen, E. N. In *Comprehensive Organometallic Chemistry II*; Wilkinson, G.; Stone, F. G. A.; Abel, E. W.; Hegedus, L. S., Eds.; Pergamon: New York, NY, 1995; Vol. 12, Chapter 11.1.
- (4) Katsuki, T. Catalytic Asymmetric Oxidations Using Optically Active (Salen)manganese(III) Complexes as Catalysts. *Coord. Chem. Rev.* **1995**, *140*, 189–214.
- (5) Fan, Q.-H.; Li, Y.-M.; Chan, A. S. C. Recoverable Catalysts for Asymmetric Organic Synthesis. *Chem. Rev.* **2002**, *102*, 3385–3466.
- (6) Limberg, C. The Role of Radicals in Metal-Assisted Oxygenation Reactions. *Angew. Chem., Int. Ed.* **2003**, *42*, 5932–5954.
- (7) Corma, A.; Garcia, H. Silica-Bound Homogenous Catalysts as Recoverable and Reusable Catalysts in Organic Synthesis. *Adv. Synth. Catal.* **2006**, *348*, 1391–1412.
- (8) Fraile, J. M.; García, J. I.; Mayoral, J. A. Noncovalent Immobilization of Enantioselective Catalysts. *Chem. Rev.* **2009**, *109*, 360–417.
- (9) Larsen, A. S.; Wang, K.; Lockwood, M. A.; Rice, G. L.; Won, T.-J.; Lovell, S.; Sadilek, M.; Turecek, F.; Mayer, J. M. Hydrocarbon Oxidation by bis- μ -oxo Manganese Dimers: Electron Transfer,

Hydride Transfer and Hydrogen Atom Transfer Mechanisms. *J. Am. Chem. Soc.* **2002**, *124*, 10112–10123.

(10) Kim, S.-S.; Zhang, W.; Pinnavaia, T. J. Catalytic Oxidation of Styrene by Manganese(II) Bipyridine Complex Cations Immobilized in Mesoporous Al-MCM-41. *Catal. Lett.* **1997**, *43*, 149–154.

(11) Kuźniarska-Biernacka, I.; Silva, A. R.; Carvalho, A. P.; Pires, J.; Freire, C. Organo-Laponites as Novel Mesoporous Supports for Manganese(III) Salen Catalysts. *Langmuir* **2005**, *21*, 10825–10834.

(12) Cardoso, B.; Pires, J.; Carvalho, A. P.; Kuźniarska-Biernacka, I.; Silva, A. R.; Castro, B.; Freire, C. Mn(III) Salen Complex Immobilised into Pillared Clays by *in situ* and Simultaneous Pillaing/Encapsulation Procedures. Application in the Heterogeneous Epoxidation of Styrene. *Microporous Mesoporous Mater.* **2005**, *86*, 295–302.

(13) Kuźniarska-Biernacka, I.; Silva, A. R.; Carvalho, A. P.; Pires, J.; Freire, C. Anchoring of Chiral Manganese(III) Salen Complex onto Organo Clay and Porous Clay Heterostructure and Catalytic Activity in Alkene Epoxidation. *Catal. Lett.* **2010**, *134*, 63–71.

(14) Kuźniarska-Biernacka, I.; Pereira, C.; Carvalho, A. P.; Pires, J.; Freire, C. Epoxidation of Olefins Catalyzed by Manganese(III) Salen Complexes Grafted to Porous Heterostructured Clays. *Appl. Clay Sci.* **2011**, *53*, 195–203.

(15) Salavati-Niasari, M. Ship-in-a-bottle Synthesis, Characterization and Catalytic Oxidation of Styrene by Host (Nanopores of Zeolite-Y)/Guest ([bis(2-hydroxyanil)acetylacetonato manganese(III)]) Nanocomposite Materials (HGMM). *Microporous Mesoporous Mater.* **2006**, *95*, 248–256.

(16) Sabater, M. J.; Corma, A.; Domenech, A.; Fornés, V.; García, H. Chiral Salen Manganese Complex Encapsulated within Zeolite Y: a Heterogeneous Enantioselective Catalyst for the Epoxidation of Alkenes. *Chem. Commun.* **1997**, 1285–1286.

(17) Gong, B.; Fu, X.; Chen, V.; Li, Y.; Zou, X.; Tu, X.; Ding, P.; Ma, L. Synthesis of a New Type of Immobilized Chiral Salen Mn(III) Complex as Effective Catalysts for Asymmetric Epoxidation of Unfunctionalized Olefins. *J. Catal.* **2009**, *262*, 9–17.

(18) Gupta, K. C.; Kumar Sutar, A.; Lin, C.-C. Polymer-Supported Schiff Base Complexes in Oxidation Reactions. *Coord. Chem. Rev.* **2009**, *253*, 1926–1946.

(19) Patel, S. A.; Sinha, S.; Mishra, A. N.; Kamath, B. V.; Ram, R. N. Olefin Epoxidation Catalysed by Mn(II) Schiff Base Complex in Heterogenised-Homogeneous Systems. *J. Mol. Catal. A: Chem.* **2003**, *192*, 53–61.

(20) Mahdavi, V.; Mardani, M.; Malekhosseini, M. Oxidation of Alcohols with Tert-Butylhydroperoxide Catalyzed by Mn(II) Complexes Immobilized in the Pore Channels of Mesoporous Hexagonal Molecular Sieves (HMS). *Catal. Commun.* **2008**, *9*, 2201–2204.

(21) Brinkman, J.; Rispens, M. T.; Hage, R.; Feringa, B. L. New Manganese Catalysts for Alcohol Oxidation. *Inorg. Chim. Acta* **2002**, *337*, 75–82.

(22) Gosling, P. A.; Nolte, R. J. M. A Manganese(III) Porphyrin/Rhodium(III) Bipyridine/Formate Catalyst System for the Reductive Activation of Molecular Oxygen. *J. Mol. Catal. A: Chem.* **1996**, *113*, 257–267.

(23) Hollmann, F.; Lin, P. C.; Witholt, B.; Schmid, A. Stereospecific Biocatalytic Epoxidation: The First Example of Direct Regeneration of a FAD-Dependent Monooxygenase for Catalysis. *J. Am. Chem. Soc.* **2003**, *125*, 8209–8217.

(24) Nunes, N.; Amaro, R.; Costa, F.; Rombi, E.; Carvalho, M. A.; Neves, I. C.; Fonseca, A. M. Copper(II)-Purine Complexes Encapsulated in NaY Zeolite. *Eur. J. Inorg. Chem.* **2007**, 1682–1689.

(25) Figueiredo, H.; Silva, B.; Raposo, M. M. M.; Fonseca, A. M.; Neves, I. C.; Quintelas, C.; Tavares, T. Immobilization of Fe(III) Complexes of Pyridazine Derivatives Prepared from Biosorbents Supported on Zeolites. *Microporous Mesoporous Mater.* **2008**, *109*, 163–171.

(26) Parpot, P.; Teixeira, C.; Almeida, A. M.; Ribeiro, C.; Neves, I. C.; Fonseca, A. M. Redox Properties of (1-(2-pyridylazo)-2-naphthol)copper(II) Encapsulated in Y Zeolite. *Microporous Mesoporous Mater.* **2009**, *117*, 297–303.

(27) Neves, I. C.; Cunha, C.; Pereira, M. R.; Pereira, M. F. R.; Fonseca, A. M. Optical Properties of Nanostructures Obtained by Encapsulation of Cation Chromophores in Y Zeolite. *J. Phys. Chem. C* **2010**, *114*, 10719–10724.

(28) Neves, I. C.; Fonseca, A. M.; Costa, F.; Pereira, M. F. R.; Pescarmona, P. Noncovalent Anchoring of Hydride Tungsten Complex on Mesoporous Materials. *Stud. Surf. Sci. Catal.* **2006**, *162*, 417–424.

(29) Kuźniarska-Biernacka, I.; Biernacki, K.; Magalhães, A. L.; Fonseca, A. M.; Neves, I. C. Catalytic Behaviour of 1-(2-Pyridylazo)-2-Naphthol Transition Metal Complexes Encapsulated in Y Zeolite. *J. Catal.* **2011**, *278*, 102–110.

(30) Chavan, S. A.; Srinivas, D.; Ratnasamy, P. Oxidation of Cyclohexane, Cyclohexanone, and Cyclohexanol to Adipic Acid by a Non-HNO₃ Route over Co/Mn Cluster Complexes. *J. Catal.* **2002**, *212*, 39–45.

(31) Medina, J. C.; Gabriunas, N.; Pfiez-Mozo, E. Cyclohexene Oxidation with an Iron Cyclam-type Complex Encapsulated in Y-Zeolite. *J. Mol. Catal. A: Chem.* **1997**, *115*, 233–239.

(32) Alcón, M. J.; Corma, A.; Iglesias, M.; Sánchez, F. New Mn(II) and Cu(II) Chiral C2-Multidentate Complexes Immobilised in Zeolites (USY, MCM41): Reusable Catalysts for Selective Oxidation Reactions. *J. Mol. Catal. A: Chem.* **2003**, *194*, 137–152.

(33) Kala Raj, N. K.; Ramaswamy, A. V.; Manikandan, P. Oxidation of Norbornene over Vanadium-Substituted Phosphomolybdic Acid Catalysts and Spectroscopic Investigations. *J. Mol. Catal. A: Chem.* **2005**, *227*, 37–45.

(34) Baker, S. R.; Clissold, D. W.; McKillop, A. Synthesis of Leukotriene A₄ Methyl Ester from D-glucose. *Tetrahedron Lett.* **1988**, *29*, 991–994.

(35) Zimmermann, P.; Schmidt, R. R. Synthese von Erythro-Sphingosinen über die Azidoderivate. *Liebigs Ann. Chem.* **1988**, 663–667.

(36) Zimmermann, P.; Schmidt, R. R. Synthesis of D-Erythro-Sphingosines. *Tetrahedron Lett.* **1986**, *27*, 481–483.

(37) Kuźniarska-Biernacka, I.; Rodrigues, O.; Carvalho, M. A.; Neves, I. C.; Fonseca, A. M. Encapsulation of Manganese(III) Complex in NaY Nanoporosity for Heterogeneous Catalysis. *Appl. Organomet. Chem.* **2012**, *26*, 44–49.

(38) Figueiredo, H.; Silva, B.; Quintelas, C.; Raposo, M. M. M.; Parpot, P.; Fonseca, A. M.; Lewandowska, A. E.; Bañares, M. A.; Neves, I. C.; Tavares, T. Immobilization of Chromium Complexes in Zeolite Y Obtained from Biosorbents: Synthesis, Characterization and Catalytic Behavior. *Appl. Catal., B* **2010**, *94*, 1–7.

(39) Corma, A.; Garcia, H. Supramolecular Host-Guest Systems in Zeolites Prepared by Ship-in-a-Bottle Synthesis. *Eur. J. Inorg. Chem.* **2004**, *6*, 1143–1164.

(40) Kuźniarska-Biernacka, I.; Fonseca, A. M.; Neves, I. C. Different Methodologies for Encapsulation of Manganese Complex Bearing 1,3-Tolyltriazene Ligand into Zeolite for Oxidation Reactions. *Inorg. Chim. Acta* **2013**, *394*, 591–597.

(41) Kuźniarska-Biernacka, I.; Rodrigues, O.; Carvalho, M. A.; Parpot, P.; Biernacki, K.; Magalhães, A. L.; Fonseca, A. M.; Neves, I. C. Electrochemical and Catalytic Studies of Manganese(III) Complex with Tetradentate Schiff Base Encapsulated in NaY Zeolite. *Eur. J. Inorg. Chem.* **2013**, 2768–2776.

(42) Kuźniarska-Biernacka, I.; Carvalho, M. A.; Rasmussen, S. B.; Bañares, M. A.; Biernacki, K.; Magalhães, A. L.; Rolo, A. G.; Fonseca, A. M.; Neves, I. C. Copper(II)imida-Salen Complexes Encapsulated into NaY Zeolite for Oxidations Reactions. *Eur. J. Inorg. Chem.* **2013**, 5408–5417.

(43) Fonseca, A. M.; Gonçalves, S.; Parpot, P.; Neves, I. C. Host-Guest Chemistry of the (N,N'-diarylacetylaminide)rhodium(III) Complex in Zeolite Y. *Phys. Chem. Chem. Phys.* **2009**, *11*, 6308–6314.

(44) Salama, T. M.; Ahmed, A. H.; El-Bahy, Z. M. Y-type Zeolite-Encapsulated Copper(II) Salicylidene-p-aminobenzoic Schiff Base Complex: Synthesis, Characterization and Carbon Monoxide Adsorption. *Microporous Mesoporous Mater.* **2006**, *89*, 251–259.

- (45) Quayle, W. H.; Peeters, G.; De Roy, G. L.; Vansant, E. F.; Lunsford, J. H. Synthesis and Spectroscopic Properties of Divalent and Trivalent tris(2,2'-dipyridine)iron Complexes in Zeolite Y. *Inorg. Chem.* **1982**, *21*, 2226–2231.
- (46) Quayle, W. H.; Lunsford, J. H. Tris(2,2'-bipyridine)ruthenium(III) in Zeolite Y: Characterization and Reduction on Exposure to Water. *Inorg. Chem.* **1982**, *21*, 97–103.
- (47) Morin, S.; Ayrault, P.; Gnep, N. S.; Guisnet, M. Influence of the Framework Composition of Commercial HFAU Zeolites on their Activity and Selectivity in m-Xylene Transformation. *Appl. Catal., A* **1998**, *166*, 281–292.
- (48) Tanaka, K.; Choo, C.-K.; Komatsu, Y.; Hamaguchi, K.; Yamaki, M.; Itoh, T.; Nishigaya, T.; Nakata, R.; Morimoto, K. Characterization and Preparation of Chained Si Species in Zeolite Supercages. *J. Phys. Chem. B* **2004**, *108*, 2501–2508.
- (49) Sedlmair, C.; Gil, B.; Seshan, K.; Jentys, A.; Lercher, J. A. An in situ IR Study of the NO_x Adsorption/Reduction Mechanism on Modified Y Zeolites. *Phys. Chem. Chem. Phys.* **2003**, *5*, 1897–1905.
- (50) Dutta, B.; Jana, S.; Bera, R.; Saha, P. K.; Koner, S. Immobilization of Copper Schiff Base Complexes in Zeolite Matrix: Preparation, Characterization and Catalytic Study. *Appl. Catal., A* **2007**, *318*, 89–94.
- (51) Weiner, H.; Hayashi, Y.; Finke, R. G. Oxygenation Catalysis by all-Inorganic, Oxidation-Resistant, Dawson-Type Polyoxoanion-Supported Transition Metal Precatalysts, [(CH₃CN)_xM]ⁿ⁺ Plus P₂W₁₅Nb₃O₆₂⁹⁻ (M = Mn^{II}, Fe^{II}, Co^{II}, Ni^{II}, Cu^I, Cu^{II}, Zn^{II}). *Inorg. Chem.* **1999**, *38*, 2579–2591.
- (52) Chaudhari, K.; Bal, R.; Srinivas, D.; Chandwadkar, A. J.; Sivasanker, S. Redox Behavior and Selective Oxidation Properties of Mesoporous Titano- and Zirconosilicate MCM-41 Molecular Sieves. *Microporous Mesoporous Mater.* **2001**, *50*, 209–218.
- (53) Xu, X.; Friend, C. M. The Effect of Rhodium Environment on Oxidation Mechanism: Conversion of Norbornene to Norbornanone on Rh(111)-p(2×1)-O. *J. Am. Chem. Soc.* **1991**, *113*, 8572–8573.
- (54) Goidstein, A. S.; Beer, R. H.; Drago, R. S. Catalytic Oxidation of Hydrocarbons with O₂ or H₂O₂ Using a Sterically Hindered Ruthenium Complex. *J. Am. Chem. Soc.* **1994**, *116*, 2424–2429.
- (55) Lee, D. G.; Van den Engh, M. In *Oxidation in Organic Chemistry*; Trahanovsky, W. S., Ed.; Academic: New York, NY, 1973.
- (56) Nguyen, S. T.; Johnson, L. K.; Grubbs, R. H.; Ziller, J. W. Ring-Opening Metathesis Polymerization (ROMP) of Norbornene by a Group VIII Carbene Complex In Protic Media. *J. Am. Chem. Soc.* **1992**, *114*, 3974–3975.
- (57) Chernysheva, A. N.; Beloglazkina, E. K.; Moiseeva, A. A.; Antipin, R. L.; Zyk, N. V.; Zefirov, N. S. Co^{II} Complex of N-[2-(phenylseleno)cyclohexyl]-N-(pyridin-2-ylmethylene) Amine: Synthesis, Electrochemistry and Catalysis of Triphenylphosphine and Norbornene Oxidation by Nitrous Oxide. *Mendeleev Commun.* **2012**, *22*, 70–72.
- (58) Maghami, M.; Farzaneh, F.; Simpson, J.; Moazeni, A. Synthesis, Characterization and Crystal Structure of a Cobalt(II) Coordination Polymer with 2,4,6-tris(2-pyridyl)-1,3,5-triazine and its Use as an Epoxidation Catalyst. *Polyhedron* **2014**, *73*, 22–29.
- (59) Narayan Biswas, A.; Das, P.; Kumar Kandar, S.; Agarwala, A.; Bandyopadhyay, D.; Bandyopadhyay, P. Chiral Iron(III)-Salen-Catalyzed Oxidation of Hydrocarbons. *Catal. Commun.* **2009**, *10*, 708–711.
- (60) Sisodiya, S.; Shylesh, S.; Singh, A. P. Tin Incorporated Periodic Mesoporous Organosilicas (Sn-PMOs): Synthesis, Characterization, and Catalytic Activity in the Epoxidation Reaction of Olefins. *Catal. Commun.* **2011**, *12*, 629–633.
- (61) Leeladee, P.; Goldberg, D. P. C₇₆Cl₃₄: High Chlorination of the Inherent Chiral Fullerene with a Helical Configuration. *Inorg. Chem.* **2010**, *49*, 3083–3085.
- (62) Bhattacharjee, S.; Yang, D.-A.; Ahn, W.-S. A New Heterogeneous Catalyst for Epoxidation of Alkenes via One-Step Post-Functionalization of IRMOF-3 with Manganese(II) Acetylacetonate Complex. *Chem. Commun.* **2011**, *47*, 3637–3639.
- (63) Talsi, E. P.; Bryliakov, K. P. Chemo- and Stereoselective C–H Oxidations and Epoxidations/cis-Dihydroxylations with H₂O₂, Catalyzed by Non-Heme Iron and Manganese Complexes. *Coord. Chem. Rev.* **2012**, *256*, 1418–1434.
- (64) Bagherzadeh, M.; Zare, M. Synthesis and Characterization of NaY Zeolite-Encapsulated Mn-Hydrazone Schiff Base: an Efficient and Reusable Catalyst for Oxidation of Olefins. *J. Coord. Chem.* **2012**, *65*, 4054–4066.
- (65) Demetgül, C.; Delikanlı, A.; Sarıbiyık, O. Y.; Karakaplan, M.; Serin, S. Schiff Base Polymers Obtained by Oxidative Polycondensation and their Co(II), Mn(II) and Ru(III) Complexes: Synthesis, Characterization and Catalytic Activity in Epoxidation of Styrene. *Des. Monomers Polym.* **2012**, *15*, 75–91.
- (66) Adhikary, J.; Guha, A.; Chattopadhyay, T.; Das, D. Heterogenization of Three Homogeneous Catalysts: A Comparative Study as Epoxidation Catalyst. *Inorg. Chim. Acta* **2013**, *406*, 1–9.
- (67) Reuter, J. M.; Sinha, A.; Salomon, R. G. Rhodium Catalysis of Allylic Oxidations with Molecular Oxygen. β -Silyl-2-Cycloalkenones. *J. Org. Chem.* **1978**, *43*, 2438–2442.
- (68) Aresta, M.; Tommasi, I.; Quaranta, E.; Fragale, C.; Mascetti, J.; Tranquille, M.; Galan, F.; Fouassier, M. Mechanism of Formation of Peroxocarbonates RhOOC(O)O(Cl)(P)₃ and their Reactivity as Oxygen Transfer Agents Mimicking Monooxygenases. The First Evidence of CO₂ Insertion into the O–O Bond of Rh(η^2 -O₂) Complexes. *Inorg. Chem.* **1996**, *35*, 4254–4260.
- (69) Silva, M.; Freire, C.; de Castro, B.; Figueiredo, J. L. Styrene Oxidation by Manganese Schiff Base Complexes in Zeolite Structures. *J. Mol. Catal. A: Chem.* **2006**, *258*, 327–333.
- (70) Varkey, S. P.; Ratnasamy, C.; Ratnasamy, P. Zeolite-Encapsulated Manganese(III)salen Complexes. *J. Mol. Catal. A: Chem.* **1998**, *135*, 295–306.
- (71) Bose, S.; Pariyar, A.; Narayan Biswas, A.; Das, P.; Bandyopadhyay, P. Mild Oxidation of Hydrocarbons by tert-Butyl Hydroperoxide Catalyzed by Electron Deficient Manganese(III) Corroles. *J. Mol. Catal. A: Chem.* **2010**, *332*, 1–6.
- (72) Jones, R. Metal π Complexes with Substituted Olefins. *Chem. Rev.* **1968**, *68*, 785–806.
- (73) Li, S.; Sarkar, S.; Wayland, B. B. Methanol as a Reaction Medium and Reagent in Substrate Reactions of Rhodium Porphyrins. *Inorg. Chem.* **2009**, *48*, 8550–8558.
- (74) Zhang, R.; Mab, J.; Wang, W.; Wang, B.; Li, R. Zeolite-Encapsulated M(Co, Fe, Mn)(salen) Complexes Modified Glassy Carbon Electrodes and their Application in Oxygen Reduction. *J. Electroanal. Chem.* **2010**, *643*, 31–38.
- (75) Bania, K. K.; Deka, R. C. Zeolite-Y Encapsulated Metal Picolinato Complexes as Catalyst for Oxidation of Phenol with Hydrogen Peroxide. *J. Phys. Chem. C* **2013**, *117*, 11663–11678.